PI 1109120

THE UNITED STATES OF AMERICA

TO ALL TO WHOM THESE PRESENTS SHALL COME:

UNITED STATES DEPARTMENT OF COMMERCE
United States Patent and Trademark Office

January 06, 2004

THIS IS TO CERTIFY THAT ANNEXED HERETO IS A TRUE COPY FROM THE RECORDS OF THE UNITED STATES PATENT AND TRADEMARK OFFICE OF THOSE PAPERS OF THE BELOW IDENTIFIED PATENT APPLICATION THAT MET THE REQUIREMENTS TO BE GRANTED A FILING DATE.

APPLICATION NUMBER: *60/422,870*
FILING DATE: *November 01, 2002*
RELATED PCT APPLICATION NUMBER: *PCT/US03/34789*

By Authority of the
COMMISSIONER OF PATENTS AND TRADEMARKS

M. Sias

M. SIAS
Certifying Officer

PRIORITY DOCUMENT
SUBMITTED OR TRANSMITTED IN
COMPLIANCE WITH
RULE 17.1(a) OR (b)

60422870.110102

Please type a plus sign (+) inside this box → [+]

PTO/SB/16 (8-00)
Approved for use through10/31/2002 OMB 0851-0032
U S Patent and Trademark Office, U S DEPARTMENT OF COMMERCE
Under the Paperwork Reduction Act of 1995, no persons are required to respond to a collection of information unless it displays a valid OMB control number

PROVISIONAL APPLICATION FOR PATENT COVER SHEET

This is a request for filing a PROVISIONAL APPLICATION FOR PATENT under 37 CFR 1.53(c).

11/01/02 11056 U.S. PTO

60422870 U.S. PTO 11/01/02

INVENTOR(S)		
Given Name (first and middle [if any])	Family Name or Surname	Residence (City and either State or Foreign Country)
Bruce J. Steven J.	Gluckman Schiff	Arlington, VA Chevy Chase, MD

☐ *Additional inventors are being named on the ___ separately numbered sheets attached hereto*

TITLE OF THE INVENTION (280 characters max)

METHODS AND DEVICES FOR PREDICTING SEIZURES

Direct all correspondence to: **CORRESPONDENCE ADDRESS**

☐ Customer Number [ ] → *Place Customer Number Bar Code Label here*

OR *Type Customer Number here*

☑ Firm or Individual Name	Jennifer Murphy				
Address	George Mason University, Office of Technology Transfer				
Address	4400 University Drive, MSN 3A2				
City	Fairfax	State	VA	ZIP	22030
Country		Telephone		Fax	

ENCLOSED APPLICATION PARTS *(check all that apply)*

☒ Specification *Number of Pages* 17 ☐ CD(s), Number

☒ Drawing(s) *Number of Sheets* 5 ☐ Other (specify)

☐ Application Data Sheet. See 37 CFR 1.76

METHOD OF PAYMENT OF FILING FEES FOR THIS PROVISIONAL APPLICATION FOR PATENT

☒ Applicant claims small entity status. See 37 CFR 1.27.

☒ A check or money order is enclosed to cover the filing fees

☐ The Commissioner is hereby authorized to charge filing fees or credit any overpayment to Deposit Account Number [ ]

☐ Payment by credit card. Form PTO-2038 is attached

FILING FEE AMOUNT ($): 80.00

The invention was made by an agency of the United States Government or under a contract with an agency of the United States Government.

☒ No

☐ Yes, the name of the U S Government agency and the Government contract number are _____

Respectfully submitted,

SIGNATURE _____

TYPED or PRINTED NAME Richard M. Lebovitz

TELEPHONE _____

Date 11/1/02

REGISTRATION NO. *(if appropriate)* 37,067

Docket Number GMU

USE ONLY FOR FILING A PROVISIONAL APPLICATION FOR PATENT

This collection of information is required by 37 CFR 1.51. The information is used by the public to file (and by the PTO to process) a provisional application. Confidentiality is governed by 35 U.S.C. 122 and 37 CFR 1.14. This collection is estimated to take 8 hours to complete, including gathering, preparing, and submitting the complete provisional application to the PTO. Time will vary depending upon the individual case. Any comments on the amount of time you require to complete this form and/or suggestions for reducing this burden, should be sent to the Chief Information Officer, U.S. Patent and Trademark Office, U.S. Department of Commerce, Washington, D.C. 20231. DO NOT SEND FEES OR COMPLETED FORMS TO THIS ADDRESS. SEND TO: Box Provisional Application, Assistant Commissioner for Patents, Washington, D.C. 20231

PTO/SB/17 (11-00)
Approved for use through 10/31/2002 OMB 0651-0032
U S Patent and Trademark Office, U S DEPARTMENT OF COMMERCE
Under the Paperwork Reduction Act of 1995, no persons are required to respond to a collection of information unless it displays a valid OMB control number

FEE TRANSMITTAL for FY 2001

Patent fees are subject to annual revision

TOTAL AMOUNT OF PAYMENT ($) 80.00

Complete if Known	
Application Number	
Filing Date	
First Named Inventor	Gluckman
Examiner Name	
Group Art Unit	
Attorney Docket No	GMU

METHOD OF PAYMENT

1. ☐ The Commissioner is hereby authorized to charge indicated fees and credit any overpayments to
   Deposit Account Number:
   Deposit Account Name:
   ☐ Charge Any Additional Fee Required Under 37 CFR 1 16 and 1 17
   ☒ Applicant claims small entity status See 37 CFR 1 27
2. ☑ Payment Enclosed: ☑ Check ☐ Credit card ☐ Money Order ☐ Other

FEE CALCULATION

1. BASIC FILING FEE

Large Entity Fee Code	Large Entity Fee ($)	Small Entity Fee Code	Small Entity Fee ($)	Fee Description	Fee Paid
101	710	201	355	Utility filing fee	
106	320	206	160	Design filing fee	
107	490	207	245	Plant filing fee	
108	710	208	355	Reissue filing fee	
114	150	214	75	Provisional filing fee	80.00

SUBTOTAL (1) ($) 80.00

2. EXTRA CLAIM FEES

	Extra Claims		Fee from below	Fee Paid
Total Claims		-20** =		x =
Independent Claims		- 3** =		x =
Multiple Dependent				=

Large Entity Fee Code	Large Entity Fee ($)	Small Entity Fee Code	Small Entity Fee ($)	Fee Description
103	18	203	9	Claims in excess of 20
102	80	202	40	Independent claims in excess of 3
104	270	204	135	Multiple dependent claim, if not paid
109	80	209	40	** Reissue independent claims over original patent
110	18	210	9	** Reissue claims in excess of 20 and over original patent

SUBTOTAL (2) ($)

**or number previously paid, if greater, For Reissues, see above

FEE CALCULATION (continued)

3. ADDITIONAL FEES

Large Entity Fee Code	Large Entity Fee ($)	Small Entity Fee Code	Small Entity Fee ($)	Fee Description	Fee Paid
105	130	205	65	Surcharge - late filing fee or oath	
127	50	227	25	Surcharge - late provisional filing fee or cover sheet	
139	130	139	130	Non-English specification	
147	2,520	147	2,520	For filing a request for *ex parte* reexamination	
112	920*	112	920*	Requesting publication of SIR prior to Examiner action	
113	1,840*	113	1,840*	Requesting publication of SIR after Examiner action	
115	110	215	55	Extension for reply within first month	
116	390	216	195	Extension for reply within second month	
117	890	217	445	Extension for reply within third month	
118	1,390	218	695	Extension for reply within fourth month	
128	1,890	228	945	Extension for reply within fifth month	
119	310	219	155	Notice of Appeal	
120	310	220	155	Filing a brief in support of an appeal	
121	270	221	135	Request for oral hearing	
138	1,510	138	1,510	Petition to institute a public use proceeding	
140	110	240	55	Petition to revive - unavoidable	
141	1,240	241	620	Petition to revive - unintentional	
142	1,240	242	620	Utility issue fee (or reissue)	
143	440	243	220	Design issue fee	
144	600	244	300	Plant issue fee	
122	130	122	130	Petitions to the Commissioner	
123	50	123	50	Processing fee under 37 CFR 1 17(q)	
126	180	126	180	Submission of Information Disclosure Stmt	
581	40	581	40	Recording each patent assignment per property (times number of properties)	
146	710	246	355	Filing a submission after final rejection (37 CFR § 1 129(a))	
149	710	249	355	For each additional invention to be examined (37 CFR § 1 129(b))	
179	710	279	355	Request for Continued Examination (RCE)	
169	900	169	900	Request for expedited examination of a design application	
Other fee (specify)					

*Reduced by Basic Filing Fee Paid SUBTOTAL (3) ($)

SUBMITTED BY				Complete (if applicable)	
Name (Print/Type)	Richard M. Lebovitz	Registration No (Attorney/Agent)	37,067	Telephone	
Signature				Date	November 1, 2002

WARNING: Information on this form may become public. Credit card information should not be included on this form. Provide credit card information and authorization on PTO-2038.

Burden Hour Statement This form is estimated to take 0 2 hours to complete Time will vary depending upon the needs of the individual case Any comments on the amount of time you are required to complete this form should be sent to the Chief Information Officer, U S Patent and Trademark Office, Washington, DC 20231. DO NOT SEND FEES OR COMPLETED FORMS TO THIS ADDRESS SEND TO Assistant Commissioner for Patents, Washington, DC 20231

METHODS AND DEVICES FOR PREDICTING SEIZURES

This application is related to U.S. Serial No. 09/729,929, filed December 6, 2000, which is hereby incorporated by reference in its entirety.

BACKGROUND

Although control system technology has made extraordinary advances during the past century, our efforts to apply sophisticated control strategies to epilepsy have been limited. Such limitations arise both from the lack of a flexible control parameter that would permit us to rapidly and reversibly increase or decrease activity in brain, and the lack of stimulation and recording amplifiers designed for simultaneous monitoring of neuronal activity during control stimulation. Uninterrupted monitoring would enable a control system to utilize ongoing information about the dynamics to prescribe the control perturbations as continuous feedback. The application of continuous feedback would allow a controller to selectively modify specific patterns of neuronal activity while minimizing the impact on other more normal activities. This approach is in contrast to 'reversible lesions' associated with high frequency stimulation, which more indiscriminately suppress neuronal activity in the neighborhood of stimulation. We here demonstrate In Vivo some technical solutions required for future implementation of continuous feedback control of seizures using electric field stimulation.

Early strategies for controlling epileptic seizures through electrical stimulation focused on stimulating sites in the brain distant from the presumed epileptic focus. Such indirect stimulation made use of the cerebellum, but initially encouraging reports (1) were difficult to replicate (2). Favorable reports of stimulation of the centromedian nucleus of the thalamus (3,4) were difficult to replicate in a controlled setting (5), and a recent controlled trial failed to demonstrate a return to baseline seizure frequency following stimulation (6). Recently, anecdotal reports of stimulation of the subthalamic nucleus for epilepsy have been reported (7,8,9). Further deep brain structures that are candidates for indirect stimulation are being explored in laboratory settings (10,11).

Another indirect stimulation strategy has been directed at stimulation of cranial nerves, especially the vagus (12). The efficacy of this technique in long term studies falls short of the expectations for resective treatment (13,14), and recently the physiological foundation for this technique has been questioned (15). Alternative cranial nerves for stimulation are being explored in laboratory settings (16,17).

Developing the technical capability for direct interaction with an epileptic focus has been an attractive subject for both laboratory and clinical investigation. As a medical therapy, direct interaction offers the prospect of a highly targeted treatment that, through spatial confinement, would limit side effects. Various laboratory studies have investigated focal drug delivery systems (18,19), and recently focal cooling (20,21).

A growing body of experimental data has also examined the prospect of direct electrical stimulation to suppress seizures. In In Vitro slice experiments, stimulation was shown to inhibit seizure formation in a manner similar to the effects of interictal burst firing activity (22,23), and the low frequency range that will produce this effect seems narrow (24). Reports of In Vivo chronic post-stimulus suppressive effects of low

frequency pulsatile stimulation (25) were found related to low level direct current (DC) leakage and may have been associated with tissue damage (26).

There have been several reports of direct stimulation of human epileptic foci In Vivo. Continuous stimulation over 2-3 weeks appeared to suppress seizures (27), and an uncontrolled report of chronic hippocampal stimulation showed similar results (28). Most recently, trains of pulse stimulation were found to suppress afterdischarges during cortical mapping (29,30).

All of these efforts have employed traditional pulse stimulation, usually with charge balanced biphasic waveforms with short (millisecond) duration. Such stimulation clearly interacts with ongoing neural activity, and there are well established safety guidelines for such stimuli (31,32). Although individual bipolar pulses may generate time-locked impulses of action potentials, recent experimental work suggests that trains of sustained large amplitude stimuli induce depolarization block of neuronal activity (33). Importantly, the large instantaneous electric currents and potentials associated with pulsatile stimuli generally preclude simultaneous monitoring of neural activity, so that continuous feedback based on the epileptic brain activity is not possible.

We have been investigating the prospect of using continuous electric fields and currents to modulate epileptic activity. In contrast to pulsatile stimulation, continuous electric field stimulation provides a means for either excitatory or suppressive modulation of ongoing neural activity depending on field sign, and the response is graded with respect to field amplitude. Importantly, electric fields can be applied without interfering with simultaneous monitoring of neural activity. In principle, control systems based on continuous electric field stimulation would supply only the current needed to modify a pathological neuronal activity and thereby minimize risk of tissue damage and minimize impact on other behaviors.

There is a long history of using polarized electric fields or currents to modulate neural activity (see for example, 34, 35, 36), and the mechanism for electric field modulation is well understood (37,38,39,40). Small electric fields polarize neurons with long asymmetric dendritic trees, shifting their somatic transmembrane potentials and making the neurons either closer to or further from threshold for action potential initiation. The magnitude and sign of the polarization is proportional to the field amplitude and sign. In contrast to pulse stimulation, electric fields can therefore be applied in a true subthreshold fashion, biasing up or down the response of neurons to their native inputs.

In earlier work, we demonstrated that small DC fields could reversibly modulate interictal activity in a graded fashion and suppress or excite epileptiform events (41). Ghai, et al. (42) demonstrated that not only were electrographic epileptiform events suppressed with DC field application, but that the associated variations in extracellular potassium during such events were also suppressed. We have recently shown that electric fields applied adaptively in a feedback loop incorporating simultaneous monitoring of neural activity can control In Vitro seizures (43). We here report the first results from establishing suitable electrode geometries and trajectories, as well as stimulation and recording electronics, required to translate these In Vitro results to In Vivo use.

DESCRIPTION OF THE INVENTION

The present invention relates to methods and devices for detecting a preseizure and/or an impending seizure in a neural system by analyzing the system's response to a stimulus or perturbation.

For example, the present invention relates to methods and devices for detecting an impending seizure and/or preseizure in a neural system, comprising one or more of the following steps, e.g., applying a stimulus to a neural system, detecting the response of the neural system to the stimulus, and determining whether the response is different from a response during the interictal state.

The stimulus can be of any kind, e.g., electrical or other physical stimulus, that produces a characteristic response upon perturbation of a neural system in a preseizure state or when a seizure is impending. It can comprise one or more components. For example, a stimulus can be an electrical stimulus presented in any effective form, e.g., as an electrical field, electrical potential difference, electric current, etc. The electrical stimulus can be of any amount or charge that is effective for probing and eliciting information about the state of the neural system. In the examples below, a subthreshold full-wave having both positive (excitatory) and negative (suppressive) components was administered to a neural system. When an excitatory response not normally observed during the interictal state was detected, this was followed by a full-blown seizure episode, indicating that it was a signal or sign of an imminent seizure. The excitatory response, or any other signal detected after an appropriate stimulus is delivered to a neural system, can be used in accordance with the present invention to detect and warn of an impending seizure. Moreover, once the signal alerts that a seizure is imminent, appropriate measures can be taken to intervene in the seizure episode, e.g., by treating and/or suppressing it (e.g., using an epilepsy control device as described in U.S. Serial No. 09/729,929, filed December 6, 2000), or by taking precautionary measures so that the subject is not injured during it.

Methods

This work was performed in accordance with NIH vertebrate animal guidelines with approval of the George Mason University Animal Care and Use Committee.

Materials and Electronics

Surgical Procedures. Male Sprague-Dawley rats (average 284g; 65 days old) were anaesthetized with a Ketamine/Xylazine (KX) mixture of 100 mg/ml Ketamine with 20 mg/ml Xylazine in a ratio of 8:1 by volume, administered in doses of 0.1 ml/100 g. Once the animal was areflexive (determined by toe or tail pinch), it was stabilized with ear and incisor bars. Additional doses of KX were administered throughout the experiment to maintain areflexia. Core temperature was monitored with a rectal thermometer and controlled with a heating pad. A vertex incision was made to expose the skull from the anterior frontal bone to the external occipital crest. A 4 mm wide craniotomy was performed bilaterally from the coronal to the lambdoid sutures leaving a 2 mm strip of bone over the sagittal sinus intact. The dura mater covering the left hemisphere was opened exposing the neocortex. A left neocortical window was created with aspiration in order to enter the body of the lateral ventricle and expose the dorsal surface of the hippocampus. On the right, a small opening was created in the center of the dura for stereotactic electrode insertion. Both exposed brain areas were kept moist with a layer of artificial cerebrospinal fluid (ASCF) containing (in mM): 155 Na^+, 136 Cl^-, 3.5 K^+, 1.2 Ca^{2+}, 1.2 Mg^{2+}, 1.25 PO_4^{2-}, 24 HCO^{3-}, 1.2 SO_4^{2-} and 10 dextrose.

Recording electronics. Field potential recordings were made from differential microelectrode pairs (tungsten, 3 MΩ impedance, fixed 240 μm spacing, Frederic Haer Corporation). Two electrode pairs were inserted into the body of the left hippocampus to a depth of ~0.2 mm. A third recording electrode was stereotactically inserted through the right neocortex into the body of the right hippocampus. An additional agar bridge electrode placed in contact with the ACSF fluid layer in the left cortical window served as measurement ground. A photograph and schematic of electrode placements are shown in Figure 1. Signals from the microelectrode pairs were differentially preamplified with custom-built headstages (gain 10), then conditioned using a standard amplifier bank (EX4-400, Dagan Corporation) with additional gains of 20-100 and bandpass filtered with high-pass frequency of 3-5 Hz and low-pass of 3 kHz. Each signal was then digitally recorded using Axon Instruments hardware and software (12 bits/sample, 5 kHz; DigiData 1200a, Axoscope).

Field potentials were recorded differentially using closely spaced electrode pairs in order to minimize the effect of the applied electric field. The custom differential preamplifiers (based on instrumentation amplifiers Analog Devices AMP02 or Texas Instrument INA116) accommodated common-mode signals between the recording electrodes and measurement ground produced by the applied electric field.

Stimulation Electrodes and Electronics. A large-scale electric field was applied by driving current between two electrodes in electrical contact with the tissue. A rod shaped depth electrode (Ag-AgCl, 0.25 mm diameter) was inserted along the central axis of the left hippocampus to a depth of ~3 mm and referenced to a circular plate electrode (2 mm diameter Ag-AgCl) placed in the ACSF layer near the left hippocampus within the cortical window. The electric field from such an axially placed cylindrical electrode is approximately radial, falls off inversely proportional to the distance from the long axis, and modulates large regions of CA3, CA2, and CA1 pyramidal neurons. An analytic approximation of the field, based on a uniform tissue conductivity of 125 Ωcm (44), is illustrated in Figure 2.

The stimulation current was created by a voltage-to-current amplifier with transformer-coupled isolation of both input and power (using an Analog Devices AD210). This allows the stimulation electrode potentials to float with respect the measurement 'ground'. Control signals were produced with a waveform generator (Hewlett Packard 33120A). The stimulation electronics are shown schematically in Figure 1.

Experimental Protocol

Overview. A 0.25 mm (o.d.) cannula for the injection of kainic acid (KA) (OPIKA-1™ Kainic Acid, Ocean Produce International) was inserted stereotactically into the right hippocampal CA1 (5.6 mm posterior to bregma, 4.5 mm lateral, and 3.0 mm deep to the cortical surface) through the dural window and intact cortex. A microperfusion pump was used to introduce 0.55 µl of 200 ng/µl KA into the hippocampus, repeated if needed at 20 min intervals (one to six applications) until epileptiform activity was observed. In 1 experiment, placing the KA loaded cannula into the CA1 was sufficient to provoke epileptiform activity and no bolus injections were administered. Following the experiments animals were euthanized with an overdose of anesthesia (0.4-0.6 ml KX).

Electric field Stimulation: Electric field stimulation was applied with either sinusoidal or multi-phase square-waves (phasic) with varying amplitudes and periods. The phasic waveform was constructed with consecutive plateaus of amplitude [0,1,0,-1] each of equal duration (see Figure 3) and connected smoothly to minimize frequency components above 25 times the waveform frequency. Afterward, other continuous waveforms, notably long DC pulses, were also applied for exploratory purposes.

Analysis

Averages values are presented as mean ± standard deviation.

Peri-stimulus RMS: Recordings (baseline and during stimulation) were digitally bandpass filtered with a second order Chebyshev filter (high-pass 10-20 Hz, low-pass 2 kHz) to remove residual stimulus artifact. We quantified the degree of modulation with the root mean squared (RMS) power in the pass band from the field potential recordings. The average RMS is calculated in half overlapping 200 ms windows.

RMS per Phase: For the phasic stimuli, the RMS activity, σ, was calculated for each phase of the stimulus for measurements in both the stimulated and the KA hippocampus (electrodes R1 and R3 respectively). To further quantify the modulation of activity by the electric field as the ongoing activity changes, the normalized RMS deviation $\Delta = (\sigma - \bar{\sigma}_z)/\bar{\sigma}_z$, was calculated, where σ is the RMS activity averaged over either the positive or the negative phase of the stimulus, and $\bar{\sigma}_z$ is the RMS activity averaged over the previous and subsequent zero-amplitude phases of the stimulus.

Seizure onset times: Seizure onset times were defined when σ for all stimulation phases on the KA side (electrode R3) exceeded threshold for 2 seconds. The threshold was chosen at a convenient value that eliminated false positives. We found that it was

possible to define a preseizure onset time when σ exceeded the same threshold for just one phase of the phasic waveform over at least 2 waveform periods.

Histology: Following euthanasia, the brain was removed intact and fixed in 4% paraformaldehyde, then sectioned and stained with hematoxylin and eosin (H&E) to establish electrode placement and examine the tissue histologically. Basic histological analysis was performed to determine the stimulation electrode trajectory and screen for evidence of acute damage to the tissue. In each of the histological slices, the position of the electrode track was identified by local tissue disruption. This position was then sketched along with gross anatomical structure and major cell body layers and mapped onto reference images derived from the Paxinos and Watson rat brain atlas (45). Reconstructed electrode positions in intermediate reference images were then plotted by linear interpolation.

Results

Interictal modulation

Electrical field modulation of ongoing hippocampal activity from the stimulated hippocampus is shown in Figure 3. Shown are examples of the different stimuli and typical responses for each of the six experiments. Baseline traces represent activity in each experiment either immediately preceding or following electrical field application. Stimuli characteristics and recording electrode identification for this figure are summarized in Table 1.

Peristimulus RMS activity for each period of sinusoidal or phasic stimulus in the traces is shown in the power analysis. Vertical axes at the right are RMS power in dB referenced to the average RMS power calculated in 200 ms windows from 10 s of baseline data recorded near in time to each stimulation protocol. The standard deviation (STD) of the average baseline RMS $STD_{baseline}$ power is marked with a left-heading hash mark (-) on the power axes, and can be used as guide to estimate significance of the variations observed during stimulation. In each case, the maximum per period variation observed during stimulation is many times the baseline STD. This normalized deviation $(RMS_{max} - RMS_{baseline})/STD_{baseline}$, averaged over experiments, is 60 ± 14 for sinusoidal and 136 ± 55 for phasic stimuli.

In 5/6 experiments RMS analysis revealed significant increase of activity at the positive and/or negative phase of the sinusoidal field. The neural response to particular phases of stimulation varied between experiments. In experiment 1 (row 1, Fig. 3) we observed an increase in activity and RMS at both the positive and negative phases of the sinusoid. Stimulus artifact from experiment 2 could not be successfully removed from the recordings so results were indeterminate. In experiments 3-6, excitation of the ongoing neural activity occurred at a single phase of the stimulation.

Similar results are seen for the phasic stimulation. Excitation occurs at both the positive and negative phases of stimulation in experiments 1, 2 and 4. Experiment 3 demonstrated excitation almost exclusively on the negative phase of stimulation. The last two experiments, 5 and 6, demonstrated both excitation on the positive phase of

stimulation and suppression of activity on the negative phase of the stimulation. This is quantified below for a longer period from experiment 5 (Figure 4).

Modulation prior to seizure onset

In two experiments (1 and 5), we observed characteristic changes in the neuronal response to stimulation in advance of the electrographic seizures.

An example from experiment 5 of bilateral activity modulation is shown in Figure 4 for 25 minutes of phasic electric field stimulation (period 2 s, amplitudes 0.29, 0.33 and 0.50 mA). We calculated the RMS activity per phase, σ, for each 0.5 s phase of the stimulus for measurements in both the stimulated and the KA hippocampus (electrodes R1 and R3 respectively). Plotted in Fig. 4A is σ for recordings in each hippocampus, with stimulus phase color encoded (color code illustrated in boxed inset). Ipsilateral to the stimulation (Stim, lower graph), the positive phase (red) yielded higher σ than either zero phase (black and green), each of which was higher than the negative phase (blue).

This pattern is intermittently interrupted by periods with increased RMS that correspond to seizures. Electrographic seizure onsets times, defined when σ exceeded a threshold (gray line) for 2 seconds (4 consecutive phases), are indicated with red arrows.

A bilateral recording of a single seizure is shown in Figure 4B. Many seconds in advance of seizure onset time, bursts of activity are observed contralateral to the stimulus starting ~350 s (upper trace). These bursts occur only on the *negative* phase of the stimulus, when the stimulated hippocampus was *suppressed.* Preseizure times defined when the activity on the KA side exceeded the same threshold as before (gray line) for two consecutive stimulus periods but only during the negative phase of the stimulus are shown with blue arrows. This preseizure onset time preceded the full onset time (red arrows) by 17 s in this example.

To further quantify the modulation of activity by the electric field as the ongoing activity changes, we introduce the normalized RMS deviation $\Delta = (\sigma - \bar{\sigma}_z)/\bar{\sigma}_z$, where σ is the RMS activity averaged over either the positive or negative phase of the stimulus, and $\bar{\sigma}_z$ is the RMS activity averaged over the previous and subsequent zero-amplitude phases of the stimulus. Excitatory modulation appears as a positive Δ and suppressive modulation as negative Δ. The normalized RMS deviation is shown in 4C for the same data as Fig 4B. On the KA side, the negative phases, shown in blue, yield a positive Δ just before the seizure onsets. This increase in activity on the KA side was repeated prior to each of the seven seizures observed in the 25 minutes of recording, shown in 4D. Preseizure onset times as defined above (blue arrows) precede full seizure onset times (red arrows) by 14 ± 2 s averaged over the seven seizures observed in the 25 minutes of this recording.

Histology

Basic histological analysis was performed to determine the stimulation electrode trajectory and screen for evidence of acute damage to the tissue. Images of histological

sections chosen from the anterior and posterior ends of the electrode track are shown for each experiment in Figure 5A.

Reconstruction of the electrode track was possible for 5/6 experiments. In experiment 2, electrode track could not be determined from the histological sections, preventing trajectory reconstruction. For experiments 1, 3 and 4, the electrode trajectory was steep and passed through the lower portion of the hippocampus. In experiments 3 and 4, it exited the ventral surface of the hippocampus.

The reconstructed electrode trajectories for experiments 5 and 6 are shown in Figure 5B. The tracks remain within the center of the hippocampus. The insertion path at the dorsal surface of the hippocampus in the CA1 region was observed in slices just anterior to the portion illustrated; trajectory positions measured in more posterior slices remained at the upper surface of the dentate gyrus. Because of the central placement of the stimulation electrode in these experiments, the electric field produced was aligned as shown in Figure 2 for a significant length of the hippocampus. These two experiments demonstrated modulation of neuronal activity proportional to the amplitude of the applied field, with positive applied field yielding excitation and negative applied field yielding suppression (Figure 3).

In 5/6 experiments, no evidence of lesioning beyond insertion damage was identified. However, in experiment 3, significant lesioning and Ag-AgCl deposition were observed along the electrode track. Tissue damage from electrodes and electrical stimulation can result from a number of mechanisms, the most common of which depends upon polarization of the electrode/fluid interface, which is a function of the unbalanced charge passed (see Table 2 for details). When the potential across this interface exceeds the oxidation/reduction (redox) thresholds for various electrolytic reactions, reaction products are created that cause lesioning (see, for example, 46). Table 2 lists the statistics of charge passage for the different experiments. The maximum unbalanced charge in experiment 3 was six times the maximum charge passed in any other experiment. The large excursions in charge passage correspond to exploratory waveforms applied after those shown in Figure 3. We note that the total charge passed, computed from the integral of the absolute value of the current, in experiments 4 and 5, in which no significant lesioning was observed, was comparable to that of experiment 3 (see Table 2 for details). The total charge passed did not appear to be the determining factor in lesioning.

Discussion

These experiments demonstrate that the use of radial electrical fields appears to be a feasible strategy for the modulation of epileptiform activity in the hippocampus. In several examples (experiments 5 and 6), modulation of ongoing activity was proportional to both the sign and amplitude of the applied field, with excitatory response observed in response to positive field and suppressive response observed in response to negative field.

The variability of the specific effects of positive or negative fields appeared related to the electrode placement with respect to the layers and geometry within the hippocampus. The two experiments (5, 6) which best demonstrated modulation

proportional to the stimulation amplitude and sign were the ones in which each electrode trajectory was confined to the central regions of the hippocampus. In these cases, we expect the electric field produced to be aligned with cell body layers as shown in Figure 2 over a significant length of hippocampus.

Such modulation with a radial field of alternating polarity is consistent with the classic work of Purpura and Malliani (36) in which surface polarization of the hippocampus increased and decreased hippocampal activity with opposite polarities as required to modulate cortex (35). These results were consistent with the geometrical inversion of the hippocampal pyramidal cells with respect to the ventricular surface compared with cortical pyramidal cells.

We observed bilateral modulation from unilateral stimulation (Fig. 4). Such observations suggest the possibility of modulating language-dominant hippocampi from non-dominant side stimuli. A further speculation would be that bilateral temporal lobe seizures might be amenable to unilateral stimulation such as this.

Whether a pre-seizure state, defined by detectable dynamical changes from baseline prior to clear seizure onset, exists and what it may be is presently a topic of considerable interest for seizure prediction and control (47, 48). We have observed that perturbations associated with periodic field stimulation can demonstrate distinctive modulation of activity prior to a seizure (Figure 4). That this modulation was observed far from the stimulus (contralateral) strongly suggests that the effect was not a measurement artifact from the stimulation. In addition, this modulation was not observed at any other time interictally except during the 14 ± 2 s prior to seizures. Such a perturbation response could be quite useful in control device design to probe for detecting dynamical changes just prior to an impending seizure. In addition, the normalized RMS deviation, Δ, could be used to detect such modulation at very low stimulation amplitudes.

The material used for our electrodes, Ag-AgCl, is unsuitable for human or chronic animal use. Fortunately, there are a number of non-toxic non-polarizing electrode materials and manufacturing options now available (49).

We observed acute lesioning in one experiment, which we attributed to extended application of DC (monopolar) current pulses that considerably polarized the stimulation electrode. Although the instantaneous current densities were low, the durations were large. We point this out specifically because lesion thresholds depend on both instantaneous current density and charge passage (see for example 50). Although there are considerable data on lesion thresholds for pulsatile stimulation (51,31,52), to our knowledge there are no data on lesion thresholds from generation of continuous electric field and related currents from electrically non-polarizing electrodes. The chronic lesion threshold will certainly be at lower charge passages than employed here and depend on electrode material. A systematic exploration of the chronic lesion threshold for lesions at electrode surfaces for continuous waveforms with zero average charge transfer will be required prior to any attempt at human trials with chronic continuous stimulation.

Our demonstration of hippocampal activity modulation with radial electric fields suggests that seizure control may be feasible with such stimulation. The next step is to develop and experimentally test control algorithms for modulation and feedback control of spontaneous seizures. The advantages of continuous electric field interaction with the

hippocampus include the possibility of minimally invasive surgical strategies employing percutaneous depth electrode insertion, in addition to subthreshold stimulation energies. Theoretically, because recording and stimulation can be made simultaneously and because the stimulation is both modulatory and graded with respect to the stimulation amplitude, it should be possible to minimize cognitive side effects. Lastly, whether a perturbation approach can serve as a useful strategy for definition and detection of a pre-seizure state is an intriguing possibility for future work.

Acknowledgements

This work was funded through a Biomedical Engineering Research Grant from the Whitaker Foundation, and through National Institutes of Health grants K02MH01493 and R01MH50006.

References

1 Cooper IS, Amin I, Riklan M, Waltz JM, Poon TP. Chronic cerebellar stimulation in epilepsy. *Arch Neurol* 1976;33:559-570.

2 Van Buren JM, Wood JH, Oakley J, Hambrecht F. Preliminary evaluation of cerebellar stimulation by double-blind stimulation and biological criteria in the treatment of epilepsy. *J Neurosurg* 1978;48:407.

3 Velasco F, Velasco M, Velasco AL, Jimenez F. Effect of Chronic Electrical Stimulation of the centromedian thalamic nuclei on various intractable seizure patterns: I. Clinical seizures and paroxysmal EEG activity. *Epilepsia* 1993;34:1052-1064.

4 Velasco F, Velasco M, Velasco AL, Jimenez F, Marquez I, Rise M. Electrical stimulation of the centromedian thalamic nucleus in control of seizures: long - term studies. *Epilepsia* 1995;36:63-71.

5 Fisher RS, Uematsu S, Krauss GL, et al. Placebo-controlled pilot study of centromedian thalamic stimulation in treatment of intractable seizures. *Epilepsia* 1992;33:841-851.

6 Velasco F, Velasco M, Jimenez F, et al. Predictors in the treatment of difficult-to-control seizures by electrical stimulation of the centromedian thalamic nucleus. *Neurosurgery* 2000;47,295-304.

7 Benabid AL, Koudsie A, Pollak P, et al. Future prospects of brain stimulation. *Neurol Res* 2000;22:237-246.

8 Benabid AL, Minotti L, Koudsie A, de Saint Martin A, Hirsch E. Antiepileptic effects of high-frequency stimulation of the subthalamic nucleus (corpus luysi) in a case of medically intractable epilepsy caused by focal dysplasia: a 30-month follow-up: technical case report. *Neurosurgery* 2002;50,1385-1392.

9 Loddenkemper T, Pan A, Neme S, et al. Deep brain stimulation in epilepsy. *J Clin Neurophysiol* 2001;18:514-532.

10 Mirski MA, Fisher RS. Electrical stimulation of the mammillary nuclei increases seizure threshold to pentylenetetrazol in rats. *Epilepsia* 1994;35,1309-1316.

11 Mirski MA, Rossell LA, Terry JB, Fisher RS. Anticonvulsant effect of anterior thalamic high frequency electrical stimulation in the rat. *Epilepsy Res* 1997;28,89-100.

12 McLachlan RS. Vagus nerve stimulation for intractable epilepsy: A review. *J Clin Neurophysiol* 1997;14:358-368.

13 Morris GL, Mueller WM. Long term treatment with vagus nerve stimulation in patients with refractory epilepsy. *Neurology* 1999;53,1731-1735.

14 DeGiorgio CM, Schachter SC, Handforth A, et al. Prospective long-term study of vagus nerve stimulation for the treatment of refractory seizures. *Epilepsia* 2000;41:1195-200.

15 Sunderam S, Osorio I, Watkins JF 3rd, Wilkinson SB, Frei MG, Davis RE. Vagal and sciatic nerve stimulation have complex, time-dependent effects on chemically-induced seizures: a controlled study. *Brain Res* 2001; 918: 60-6.

16 Fanselow EE, Reid AP, Nicolelis MA. Reduction of pentylenetetrazole-induced seizure activity in awake rats by seizure-triggered trigeminal nerve stimulation. J *Neurosci* 2000; 20: 8160-8.

17 Patwardhan RV, Tubbs RS, Killingsworth C, Rollins D, Smith WM, Ideker R. Ninth cranial nerve stimulation for epilepsy control part 1: efficacy in an animal model. *Pediatr Neurosurg*, in press.

18 Eder HG, Stein A, Fisher RS. Interictal and ictal activity in the rat cobalt/pilocarpine model of epilepsy decreased by local perfusion of diazepam. *Epilepsy Res* 1997;29:17-24.

19 Eder HG, Jones DB, Fisher RS. Local perfusion of diazepam attenuates interictal and ictal events in the bicuculline model of epilepsy in rats. *Epilepsia* 1997;38:516-521.

20 Yang XF, Rothman SM. Focal cooling rapidly terminates experimental neocortical seizures, *Ann Neurol* 2001;49:721-726.

21 Yang XF, Duffy DW, Morley RE, Rothman SM. Neocortical seizure termination by focal cooling: Temperature dependence and automated seizure detection, *Epilepsia* 2002;43:240-245.

22 Bragdon AC, Kojima H, Wilson WA. Suppression of interictal bursting in hippocampus unleashes seizures in entorhinal cortex: a proepileptic effect of lowering $[K+]_o$ and raising $[Ca2+]_o$. *Brain Res* 1992;590,128-135.

23 Barbarosie M, Avoli M. CA3-driven hippocampal-entorhinal loop controls rather than sustains In Vitro limbic seizures. *J Neurosci* 1997;17:9308-9314.

24 Jerger K, Schiff SJ. Periodic Pacing an In Vitro Epileptic Focus. 1995;73:876-879.

25 Weiss SR, Li XL, Rosen JB, Li H, Heynen T, Post RM. Quenching: inhibition of development and expression of amygdala kindled seizures with low frequency stimulation. *Neuroreport* 1995;6:2171-2176.

26 Weiss SRB, Eidsath A, Li XL, Heynen T, Post RM. Quenching revisited: low level direct current inhibits amygdala-kindled seizures. *Exp Neurol* 1998;154:185-92.

27 Velasco AL, Velasco M, Velasco G, et al. Subacute and chronic electrical stimulation of the hippocampus on intractable temporal lobe seizure: preliminary report. *Arch Med Res* 2000;31:316-328.

28 Velasco M, Velasco G, Velasco AL, et al. Subacute electrical stimulation of the hippocampus blocks intractable temporal lobe seizures and paroxysmal EEG activities. *Epilepsia* 2000;41:158-169.

29 Lesser RP, Kim SH, Beyderman, L, et al. Brief bursts of pulse stimulation terminate afterdischarges caused by cortical stimulation. *Neurology* 1999;53:2073-2081.

30 Motamedi GK, Lesser RP, Miglioretti DL, et al. Optimizing parameters for terminating cortical afterdischarges with pulse stimulation. *Epilepsia*, in press.

31 Agnew WF, Yuen TGH, McCreery DB. Morphological changes after prolonged electrical stimulation of the cat's cortex at defined charge densities. *Exp Neurol* 1983;79:397-411.

32 Gordon B, Lesser RP, Rance NE, et al. Parameters for direct cortical electrical stimulation in the human: histopathological confirmation. *Electroenecephalogr Clin Neurophysiol* 1990;75:371-377.

33 Bikson, M, Lian, J, Hahn, PJ, Stacey, WC, Sciortino, C, Durand, DM. Suppression of epileptiform activity by high frequency sinusoidal fields in rat hippocampal slices. *J. Physiol* 2001, 531, 181-191.

34 Denney, D, Brookhart, JM. The effects of applied polarization on evoked electrocortical waves in the cat. *Electroenceph. and Clin. Neurophysiol.* 1962, 14, 885-897.

35 Purpura, DP, McMurtry, JG. Intracellular activities and evoked potential changes during polarization of motor cortex. *J. Neurophysiol.* 1965, 28, 166-185.

36 Purpura DP, Malliani A. Spike generation and propagation initiated in dendrites by transhippocampal polarization. *Brain Res* 1966;1:403-406.

37 Jefferys JGR. Influence of electric fields on the excitability of granule cells in guinea-pig hippocampal slices. *J Physiol* 1981;319:143-152.

38 Chan CY, Nicholson C. Modulation by applied electric fields of Purkinje and stellate cell activity in the isolated turtle cerebellum. *J Physiol* 1986;371:89-114.

39 Chan CY, Houndsgaard J, Nicholson C. Effects of electric fields on transmembrane potential and excitability of turtle cerebellar Purkinje cells In Vitro. *J Physiol* 1988;402:751-771.

40 Tranchina D, Nicholson, C. A model for the polarization on neurons by extrinsically applied electric fields. *Biophys J* 1986;50:1139-1159.

41 Gluckman BJ, Neel EJ, Netoff TI, Ditto WL, Spano ML, Schiff SJ. Electric field suppression of epileptiform activity in hippocampal slices. *J Neurophysiol* 1996;76:4202-4205.

42 Ghai, RS, Bikson, M, Durand, DM. Effects of applied electric fields on low-calcium epileptiform activity in the CA1 region of rat hippocampal slices. *J. Neurophysiol.*, 2000, 84, 274-280.

43 Gluckman BJ, Nguyen H, Weinstein SL, Schiff SJ. Adaptive Electric Field Suppression of Epileptic Seizures. *J Neurosci* 2001;21:590-600.

44 Traub RD, Miles R. Neuronal networks of the Hippocampus. Cambridge: Cambridge Univ. Press, 1991.

45 Paxinos G, Watson C. The Rat Brain in Stereotaxic Coordinates. 3rd edition. San Diego, Academic Press, 1997.

46 Fisher AC. Electrode Dynamics. Oxford: Oxford University Press, 1996.

47 Le Van Quyen M, Martinerie J, Navarro V, Baulac M, Varela FJ. Characterizing neurodynamic changes before seizures. *J Clin Neurophysiol* 2001;18:191-209.

48 Lehnertz K, Andrezejak RG, Arnhold J, et al. Nonlinear EEG analysis in epilepsy: its possible use for interictal focus localization, seizure anticipation and prevention. *J Clin Neurophysiol* 2001;18:209-223.

49 Meyer RD, Cogan SF, Nguyen TH, Rauh RD. Electrodeposited iridium oxide for neural stimulation and recording electrodes. *IEEE Trans Neural Syst Rehabil Eng* 2001;9:2-11.

50 Weiland JD, Anderson DJ. Chronic neural stimulation with thin-film, Iridium Oxide electrodes. IEEE Trans BME 2000, 47, 911-918.

51 Babb TL, Soper HV, Lieb JP, Brown WJ, Ottino CA, Crandall PH. Electrophysiological studies of long term electrical stimulation of the cerebellum in monkeys. *J Neurosurg* 1977:47:353-365.

52 Gordon B, Lesser RP, Rance NE, et al. Parameters for direct cortical electrical stimulation in the human: histopathologic confirmation. *Electroencephalogr Clin Neurophysiol* 1990;75:371-7.

Tables

Experiment	Recording Electrode	Sinusoidal		Phasic Stimulation	
		Amplitude (mA)	Frequency (Hz)	Amplitude (mA)	Frequency (Hz)
1	R2	0.25	0.5	1.0	0.25
2	R1			0.1	0.25
3	R2	1.25	0.2	1.2	0.025
4	R2	1.0	0.5	1.2	0.05
5	R1	0.37	0.5	0.3	0.2
6	R1	0.05	1.0	0.01	0.25

Table 1: Characteristics for traces and stimuli presented in Figure 3. Traces presented were measured using electrodes R1 or R2 as shown in Figure 1. Amplitudes are peak-zero.

Experiment	Maximum Unbalanced Charge Q_{unbal} per cycle of periodic stimulus (mC)	Maximum Unbalanced Charge Q_{unbal} during experiment (mC)	Unbalanced Charge Q_{unbal} at end of experiment (mC)	Total Charge Passed Q_{pass} (mC)
1	1.0	9.7	-1.0	105
2	0.16	3.9	-3.9	105
3	15.0	57.5	-52.9	835
4	6.0	6.0	0.0	421
5	1.55	9.6	1.5	624
6	0.05	4.6	-2.9	32

Table 2: Charge passage statistics for each experiment calculated. Unbalanced Charge, $Q_{unbal}(T) = \int_{T_0}^{T} I(t)dt$, computed by integrating the applied current. Maximum Unbalanced Charge computed as the largest absolute value Q_{unbal} during one stimulus period or full experiment. Unbalanced Charge at end of experiment is computed from beginning to end of experiment. For most experiments, the periodic waveforms applied relatively low maximal charge variations. The majority of unbalanced charge came from non-periodic stimuli applied after the experiments reported here. Total Charge Passed was computed by integrated absolute value of current, $Q_{pass}(T) = \int_{T_0}^{T} |I(t)|dt$. We attribute the severe lesioning observed in experiment 3 to the maximum unbalanced charge passed, and not the total charge passed.

Figure Captions

Fig. 1: Photo of left hippocampus and hardware during experiment 4, and schematic of experimental preparation and stimulation electronics. Two recording microelectrode pairs (**R1** and **R2**) were inserted into the body of the exposed left hippocampus. A third recording microelectrode pair (**R3**) was inserted through the intact right neocortex into the right hippocampus. An agar bridge placed in contact with the ACSF fluid layer over the rostral portion of the left cortical cavity served as measurement ground. An injection cannula (**KA**) for the perfusion of kainic acid into the right hippocampus was inserted vertically into the CA1 through a dural window. The stimulation electrode was inserted along the center axis of the exposed left hippocampus while the stimulation reference plate was placed in the ACSF fluid layer in the lateral posterior region of the left neocortical window. The stimulation current was created by a voltage-to-current amplifier with transformer-coupled isolation of both input and power (using an Analog Devices AD210) programmed from a standard waveform generator.

Fig. 2: Electric field geometry and amplitude for depth electrode placed axially within hippocampus. For fixed stimulation electrodes, the geometry of the electric field is constant, while the amplitude of the field will be linearly proportional to the current applied between stimulation electrodes. (Above) Illustration of geometry of field within perpendicular midplane of electrode from analytic calculation. The field is radial, and parallel to the long dendrite-soma axis of the pyramidal neurons in large regions of both CA3 and CA1. (Below) Proportionality constant between field and applied current, based on depth electrodes used (0.25 mm diameter, 5 mm long) and uniform tissue conductivity of 125 Ωcm (44). Along the perpendicular midplane, the field should fall off proportional to $\frac{1}{rl\sqrt{1+4(r/l)^2}}$ (solution for a finite length line source), where r is the radius and l is the length of the electrode.

Fig. 3. Modulation of hippocampal field potential activity by sinusoidal and phasic radial electric field stimulation from six experiments. Traces: Field potential traces were measured from the stimulated hippocampus during baseline activity and during sinusoidal and multiphasic electrical stimulation. Calibration bars indicate field potential amplitude in mV (vertical) and time in seconds (horizontal). Amplitude and frequency of the stimuli and measurement electrode identification are listed in Table 1. The sinusoidally stimulated response trace from experiment 5 was vertically clipped for presentation. Sinusoidal and phasic response data were bandpass filtered (10-20 Hz to 2 kHz) to reduce stimulation artifact. Power analysis: Power was calculated from 200 ms half-overlapped windows with phase of stimuli overlain, and plotted in decibels (dB) relative to average baseline power ($dB = 20\log(RMS/RMS_{baseline})$) for each period of stimulus shown in the traces. One standard deviation of window-to-window baseline power fluctuation is indicated by left-heading hashmark (-) along vertical axes and can be used as an estimate of significance for observed fluctuations. One period of the stimulus is overlaid as a visual guide.

Fig. 4. Bilateral modulation between and during seizures. (Experiment 5: phasic stimulus, 2 Hz period, amplitudes: 0.29 mA 0<t<225 s, 0.33 mA 225<t<685 s, 0.50 mA 685<t<1500 s). In each panel, the lower graphs correspond to measurements or analysis from the stimulated left hippocampus (Stim), and the upper graphs correspond to the right hippocampus that received the KA injection (KA). **A** RMS Activity Per Phase, σ, during a 25 minute recording. Phase is color coded ([1,0,-1,0] : [red,green,blue,black]) as illustrated in inset above C. Interictally, σ for the stimulated hippocampus (lower graph) is typically higher during the positive phase of the stimulus (red) and lowest during the negative phase (blue). This pattern is violated during seizures. **B** Field potential traces and σ through the seizure at t=375 s. Vertical tick marks on traces correspond to 2 mV field potential deflections. Significant excitatory responses on the KA side (upper graphs) are observed during the *negative* phase (blue) of the stimulus prior to the beginning of the seizure. **C** Normalized RMS deviation $\Delta = (\sigma - \bar{\sigma}_z)/\bar{\sigma}_z$ during the positive (red) and negative (blue) phases of the stimulus for the same period as in B. Contralateral to the stimulus (KA side), this measure increased dramatically prior to the seizure. **D** Δ for the same period as in A. Contralateral to the stimulus (KA side), Δ increased for the negative phase at the beginning of each seizure. Seizure onset times (red arrows) defined when σ exceeded the threshold (gray line) for all stimulus phases on KA side for at least 2 seconds. Preseizure onset times (blue arrows) defined when σ exceeded the threshold (gray line) for two consecutive stimuli periods only during the negative stimulus phase. Preseizure onset times precede seizure onset times by 14 ± 2 s for the seven seizures observed.

Fig. 5. Histological Images and Stimulation Electrode Track Reconstruction. **A** Images from the anterior and posterior ends of the electrode trajectory for each experiment (numbered to the left), with magnified images of the electrode track shown when clearly visible (arrows). Approximate stereotaxic coordinates determined by comparison to a rat brain atlas (45). **B** Electrode path reconstruction for experiments 5 and 6. The interpolated electrode trajectory for each is indicated on the atlas reference slices with an (x). The position of recording electrode **R1** is estimated by cross-referencing surface photos from the experiment with the histological sections and the rat atlas reference. Orientational notation: L=Lateral, M=medial, A=Anterior, P=Posterior. Reproduced after reference (45) with permission from publisher.

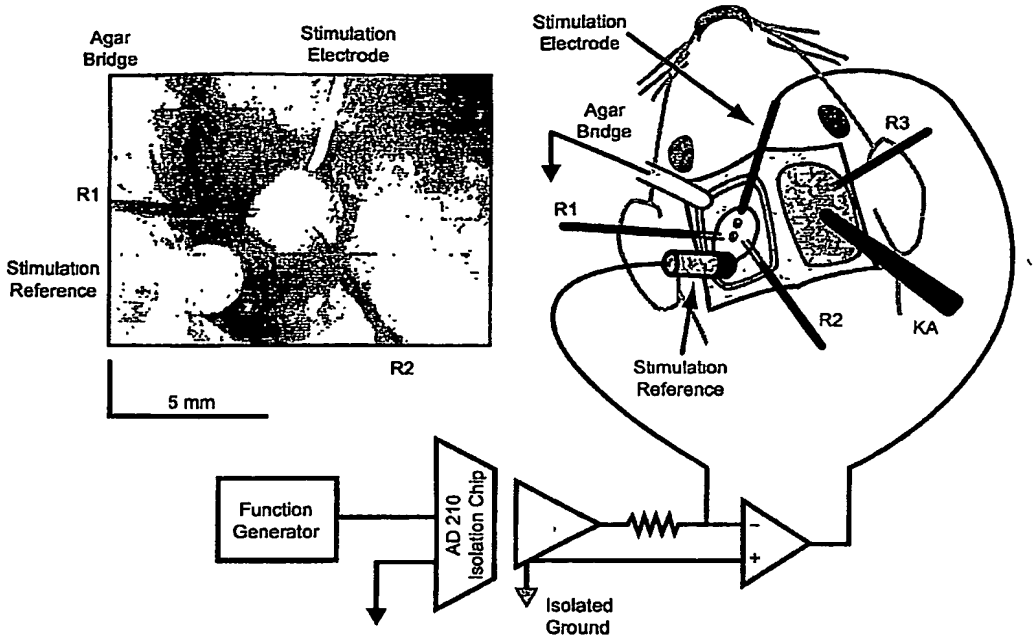

Figure 1

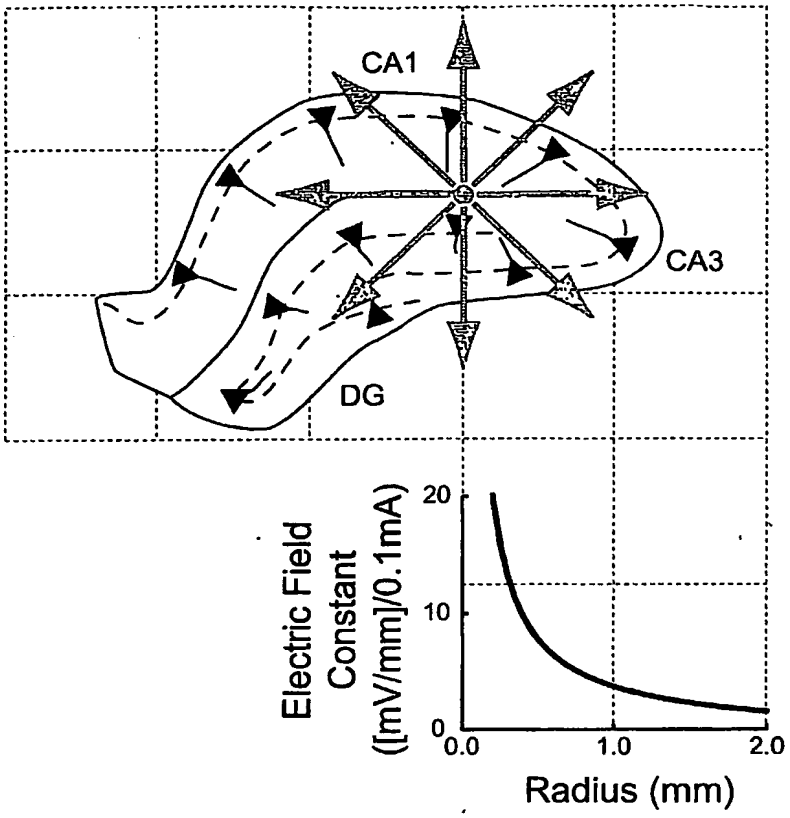

Figure 2

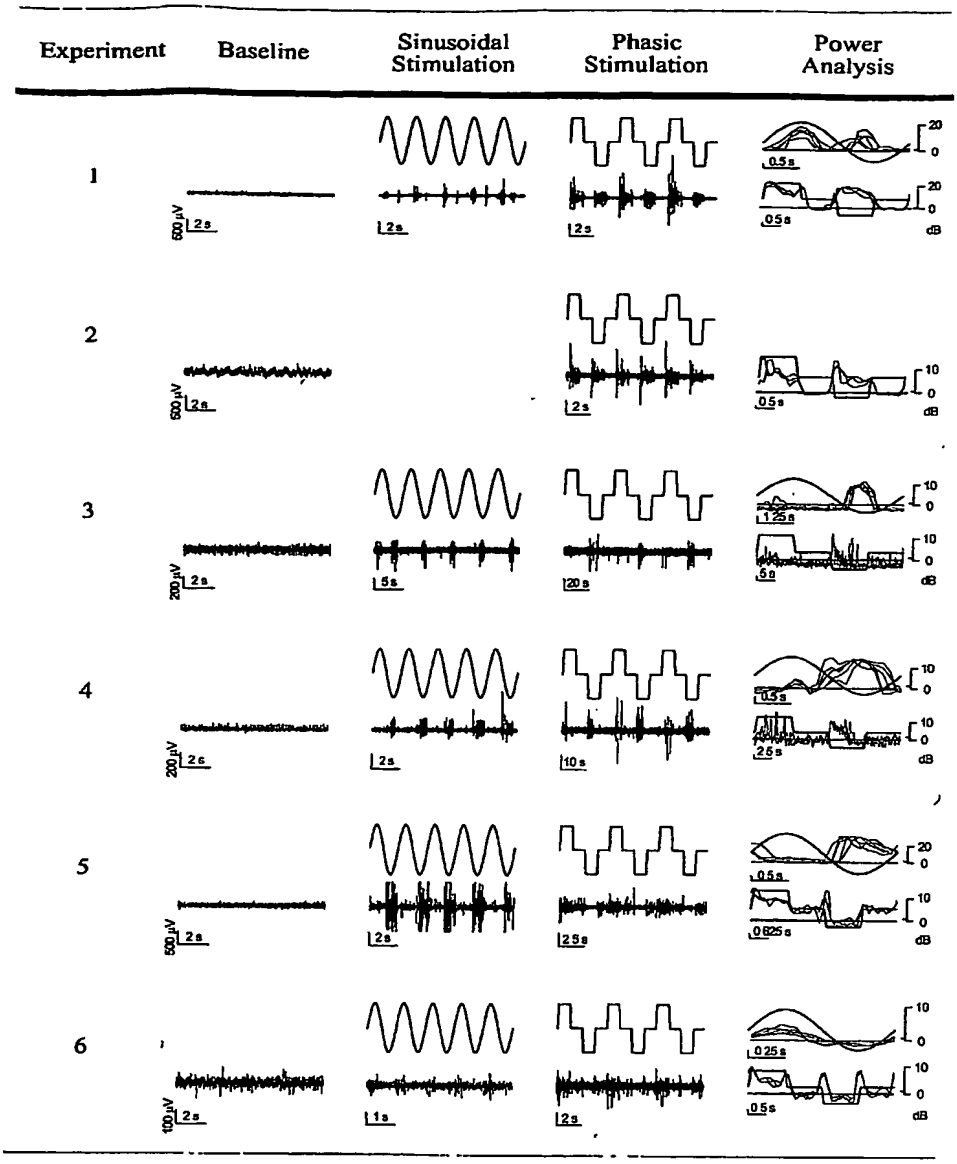

Figure 3

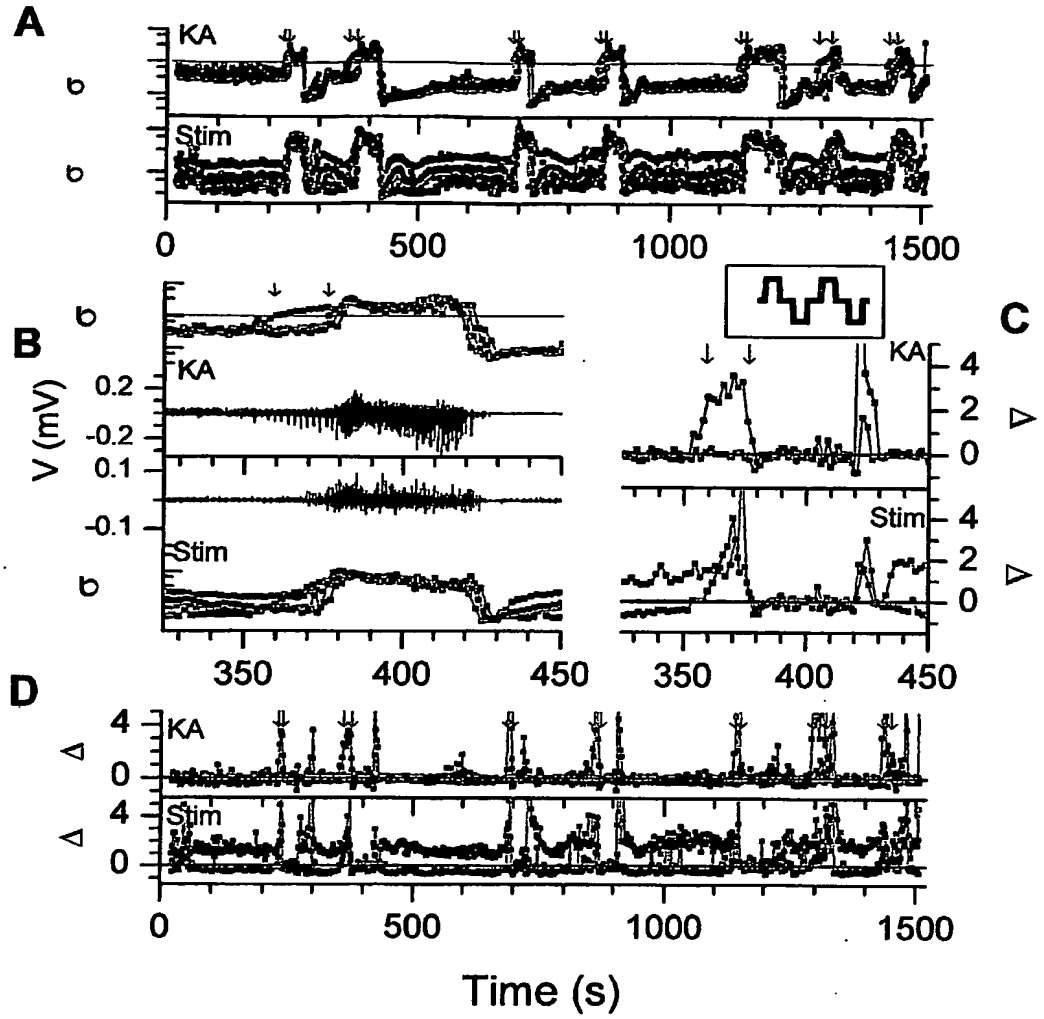

Figure 4

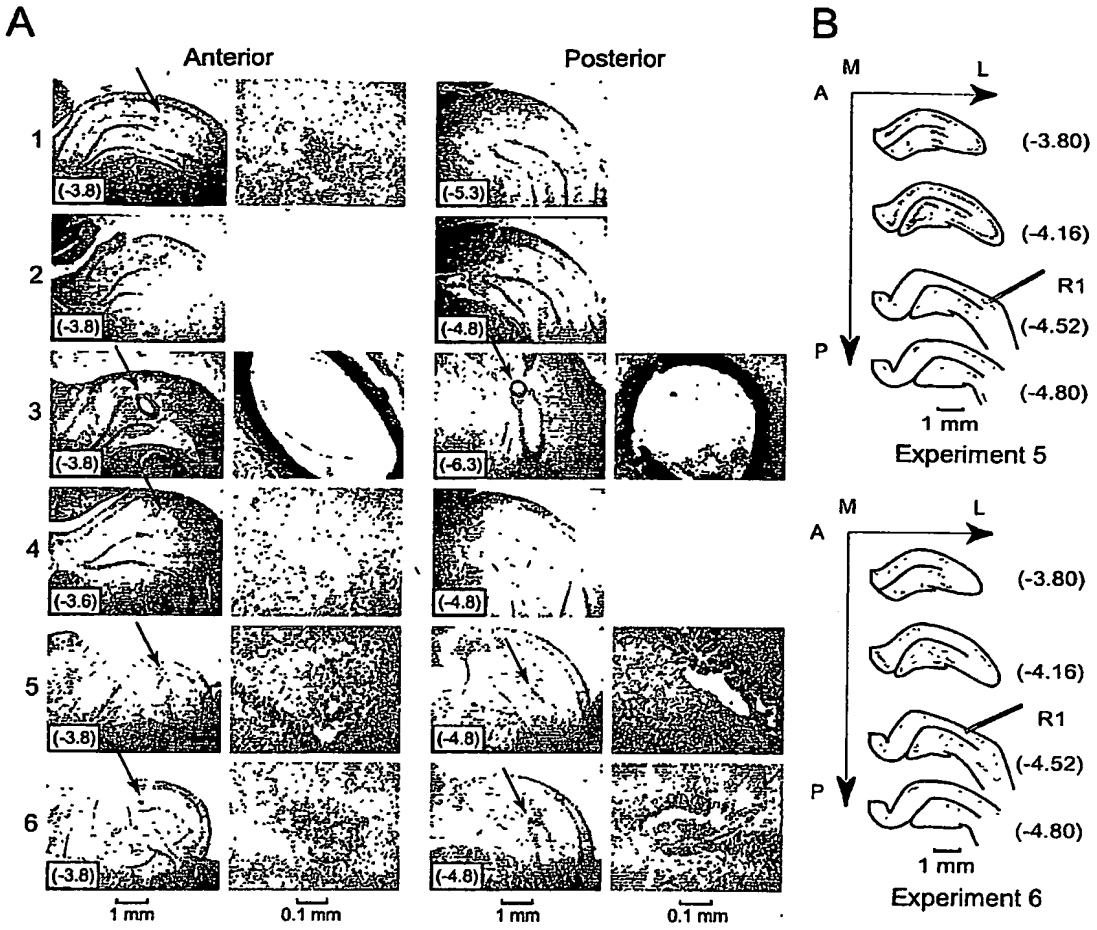

Figure 5